Geochemistry of the metagabbros of Syros.

Aaron Grandy
1787 N. 230 W. Cedar City, UT 84720
Faculty Sponsor: Stanley C. Hatfield, Southern Utah University

INTRODUCTION

Geologic History. The Greek Cyclades are a group of islands located in the Aegean Sea just southeast of Greece. Metamorphic rocks dominate this region with metamorphic grades ranging from greenschist on up to epidote-blueschist and eclogite facies (Evans,1990). The consequent cause of this metamorphism is the closing of the Tethys Sea and the formation of the Alpine orogenic belt around 45mya (Schuiling,1973). Indeed, the rocks seen in the Greek Cyclades represent the crustal roots of the Alpine orogeny and consist of blueschist/eclogite rocks. A second metamorphic episode later occurred between 20-25mya during normal regional metamorphism and is responsible for extensive greenschist overprints.

The island of Syros (along with nearby Sifnos) is comprised of the best preserved high-pressure/low temperature metamorphic rocks in the Greek Cyclades. Overall, Syros consists of northerly dipping, alternating sequences of marbles and calcareous schists, also in lesser abundance are zones and bands of meta-igneous rocks such as metagabbros, metabasalts, serpentinite, and mafic knockers commonly associated with melange units and serpentinite zones. The trend and localization of these units has led to the hypothesis that these rocks represent sections of an ophiolite sequence.

Project Description. This project focuses on the geochemistry of the coarse-grained mafic metamorphic rocks believed to have originated as gabbros. Three compositional varieties are found abundantly at specific locations on Syros; metagabbros rich in Mg, those rich in Fe/Ti and lacking in Mg, and an intermediate variety. Through collecting of five localities on Syros including, Kini (station 1), north of Ermoupoli (2), Kampos/Mega Lakkos (3), Kastri (4), and Galissas (5), (see figure 1), 24 samples of metagabbros, including both the Mg and Fe/Ti varieties were collected along with one serpentinite sample and one felsic "stringer" sample.

Through petrographic study and SEM-EDX analysis the mineral phases are characterized in order to establish whether or not the samples represent true metegabbros and to determine the metamorphic grade of the area.

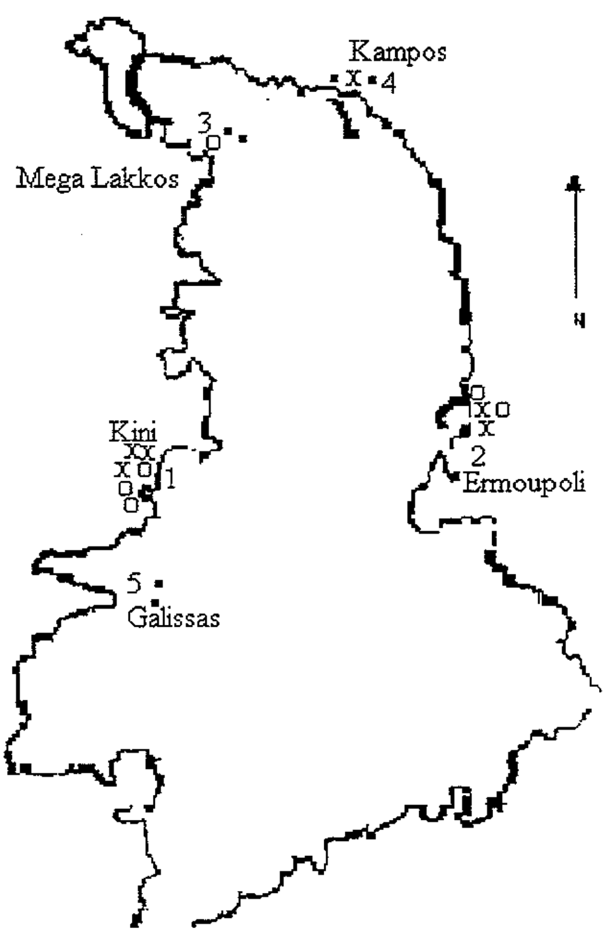

Figure 1. Map of Syros showing 5 locations with metagabbro variety sampled at each location.
X=Fe/Ti-rich, O=Mg-rich, •=intermediate composition

By use of major, trace, and rare earth analysis, the chemistry of the samples is examined and a comparison is made between protolith gabbro and the metagabbro geochemistry. From this the theory to whether or not these rocks represent gabbros is examined along with an evaluation of the effects of metasomatism.

METHODS

Field Procedures. Metagabbro samples collected from five sites on Syros (figure 1) share the following characteristics: 1)Very coarse grain sizes (ranging from 10-30mm). It is known that gabbros have large coarse crystals and once metamorphosed the metagabbros should still exhibit large crystals, although the minerals may have changed to phases stable at the P/T conditions of metamorphism; 2)All samples are representative and the least weathered material for the location. Due to the geochemical nature of this study, approximately half of the samples came directly from outcrop; it was often more convenient to collect fresh samples from float originating near the outcrops; 3)Samples are representative of both the Fe/Ti and Mg-rich metagabbros on Syros; and 4)All samples came from the most homogeneous material from each outcrop in order to get more accurate geochemical results.

Mineral Identification. Both the Mg-rich and Fe/Ti-rich metagabbros contain similiar minerals. Mg-rich metagabbros contain (in order of abundance) omphacite, blue-amphibole, phengite, chlorite, zoisite, garnet, and titanite whereas Fe/Ti-rich metagabbros contain blue-amphibole, garnet, omphacite, epidote, chlorite, phengite, rutile, and titanite. In handsample, blue-amphibole tends to be dark black in Fe/Ti-rich samples and light-blue in Mg-rich metagabbros. Omphacite was identified by its light-green to less commonly dark, neon-green color due to chromium.

In thin section the main difference between the two compositional varieties of metagabbro is color and pleochroism under plain polarized light. The minerals in Fe/Ti-rich metagabbros have increased pleochroism and color. This is particularly evident in blue-amphibole which takes on a dark blue/purple pleochroism due to high iron concentration. Blue-amphibole in Mg-rich Metagabbros has washed-out light colors.

Seven thin sections (3 Fe/Ti-rich and 4 Mg-rich metagabbros) were analyzed at Amherst College using a SEM-EDX (Energy Dispersive X-ray Analysis). This provided a means to conduct a semi-quantitative elemental analysis on the mineral phases present. The detail of the SEM made it possible to see relic igneous textures especially in what is now omphacite. Three garnet traverses were obtained and most compositional zoning occurred near the garnet rims. Coronas of chlorite, white mica, and sometimes epidote were also present around blue-amphibole and omphacite. A slight greenschist overprint was evident at this scale in some of the samples as indicated by slight alteration of omphacite and blue-amphibole to chlorite. As for white mica, phengite became distinguishable from paragonite (based on sodium content) and epidote from zoisite (based on iron).

Geochemical Analysis. 20 half kilogram samples were crushed and prepared for bulk, trace, and isotopic (ICP-MS) geochemical analysis at WSU Geoanalytical Laboratory. The original two-three kilogram samples were crushed into small chips and the most representative and unaltered chips were used in the analyses. The chemical data was manipulated into various graphs and plots using IGPET99. The assumption is made that the bulk chemistry of the metagabbros should not have altered much from the original gabbro bulk chemistry by processes such as metasomatism.

RESULTS/CONCLUSIONS

Bulk Chemical Analyses:

	2A	6A	7A	8A	4A	9A	11A	13A	14A	4B	4B-A
SiO2	50.27	49.55	52.24	51.55	56.59	45.51	48.79	52.35	52.51	52.92	43.86
Al2O3	15.52	12.52	16.22	17.29	15.57	10.89	2.78	20.52	15.52	16.34	20.09
TiO2	1.938	5.06	0.346	0.350	1.428	7.24	0.022	1.191	0.631	0.769	0.596
FeO	7.76	13.56	3.31	3.70	7.21	17.03	7.62	4.88	6.13	6.95	7.05
MnO	0.153	0.189	0.091	0.081	0.134	0.242	0.103	0.083	0.163	0.225	0.163
CaO	13.31	7.96	11.88	14.64	6.90	8.67	0.03	11.64	9.98	7.83	12.91
MgO	7.63	5.40	10.07	8.85	5.84	6.68	40.54	4.84	7.90	8.65	11.56
K2O	0.06	0.17	0.27	0.10	0.95	0.09	0.01	0.27	0.79	0.71	1.37
Na2O	3.02	5.46	5.56	3.41	5.33	3.62	0.10	4.17	6.33	5.52	2.39

	13B	14B	8C	13C	6E	6F	6G	1G	1H	6H	15
SiO2	50.64	53.32	52.14	54.19	72.60	44.98	52.77	48.14	49.37	50.52	50.38
Al2O3	13.46	15.04	16.54	15.56	16.64	10.34	16.29	12.93	13.16	20.97	17.76
TiO2	5.22	1.350	0.199	0.985	0.327	8.01	0.593	6.36	5.02	0.571	1.578
FeO*	14.04	7.76	3.41	6.36	2.94	16.78	5.52	13.83	12.34	4.45	8.28
MnO	0.234	0.153	0.116	0.135	0.014	0.225	0.121	0.199	0.214	0.096	0.160
CaO	4.99	8.60	9.59	9.77	1.63	8.93	12.35	7.88	8.39	11.44	10.34
MgO	5.65	8.75	11.24	7.44	0.45	6.76	8.79	5.74	6.22	7.77	7.34
K2O	0.42	0.10	1.40	0.42	0.62	0.05	0.06	0.25	0.72	0.19	0.16
Na2O	5.25	4.83	5.34	5.08	4.74	3.88	3.46	4.65	4.52	3.96	3.81

Trace Chemical Analyses (ppm):

	2A	6A	7A	8A	4A	9A	11A	13A	14A	4B	4B-A
Ni	43	24	196	175	47	54	2173	53	98	72	45
Cr	114	113	712	848	50	83	2633	34	48	61	33
Sc	35	55	34	34	29	59	10	19	45	54	55
V	257	869	145	142	180	1108	46	156	205	210	260
Ba	8	0	51	17	52	0	11	49	184	71	323
Rb	0	7	3	3	17	0	1	6	7	23	48
Sr	528	183	145	342	285	28	3	322	123	351	1103
Zr	166	134	14	18	104	64	5	44	31	29	29
Y	29	45	9	10	33	20	1	14	16	21	17
Nb	12.4	6.9	1.4	0.9	4.4	5.2	1.2	4.0	2.0	1.9	2.6
Ga	18	23	11	15	21	17	4	18	16	13	18
Cu	34	22	39	7	14	63	14	13	56	31	987
Zn	54	99	21	42	70	95	50	32	41	60	41
Pb	8	1	4	0	8	0	0	0	1	16	47
La	19	11	0	0	12	0	1	1	7	0	15
Ce	44	12	5	0	26	18	1	4	20	6	3
Th	2	3	1	0	2	1	1	4	0	2	3

	13B	14B	8C	13C	6E	6F	6G	1G	1H	6H	15
Ni	26	50	256	23	13	35	53	5	10	77	97
Cr	36	28	841	26	7	77	57	40	43	279	216
Sc	44	39	18	58	1	80	44	51	55	30	34
V	621	223	75	258	53	1143	183	738	822	130	228
Ba	139	19	255	130	43	0	6	7	74	10	6
Rb	19	2	20	16	19	0	0	4	18	4	2
Sr	66	167	128	138	216	116	269	123	82	263	249
Zr	87	64	49	46	766	82	37	98	96	32	127
Y	27	21	11	21	105	27	15	22	27	11	33
Nb	6.3	3.7	1.8	2.0	9.0	4.2	1.7	5.7	3.7	2.0	7.3
Ga	18	17	9	15	33	20	14	17	20	13	19
Cu	28	15	0	46	15	47	69	20	20	21	25
Zn	107	45	24	39	12	103	39	97	99	38	67
Pb	1	4	1	2	0	1	0	0	0	1	3
La	0	4	0	6	20	0	0	0	2	7	18
Ce	19	1	6	25	76	15	10	20	27	13	31
Th	2	0	1	2	2	3	0	2	0	1	3

Graphs. Figure 2 is a triangular plot of Na_2O, FeO, and MgO using the data from the bulk chemical analyses. From this graph the samples can be divided into three categories of metagabbros; 1)Fe/Ti-rich (samples 1G, 1H, 6A, 6F, 9A, 13B); 2)Intermediate (samples 4A, 4B, 13A, 13C, 14A, 14B); and 3)Mg-rich (samples 4B-a, 6G, 6H, 7A, 8A, 8C). Samples 2A and 15, which were found to be greenschist from petrologic study, both plot in the upper right field of the intermediates, sample 11A (serpentinite) plots in the far right field of the Mg-rich, and 6E (felsic stringer) plots the farthest left in the triangle. From the geochemical findings a strong correlation between high iron content and high titanium is also seen and is the basis for the classification name Fe/Ti-rich metagabbros.

Using the classification scheme presented from figure 2 and the rare-earth geochemical data, three spider (MORB) plots are presented in figure 3 to relate the findings of the rare-earth analyses which are not included in this summary. Similar depletion and enrichment trends in each category of metagabbros is evidence that the samples within each group underwent similar fractionation and share similar origins.

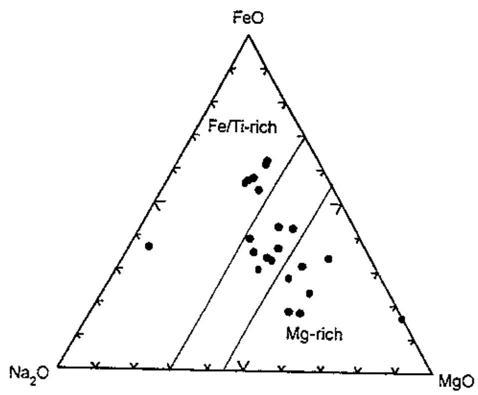

Figure 2. Triangular plot of Na_2O, FeO, MgO. From this the three compositional variaties of metagabbros are derived. Fe/Ti-rich, Intermediate, and Mg-rich metagabbros.

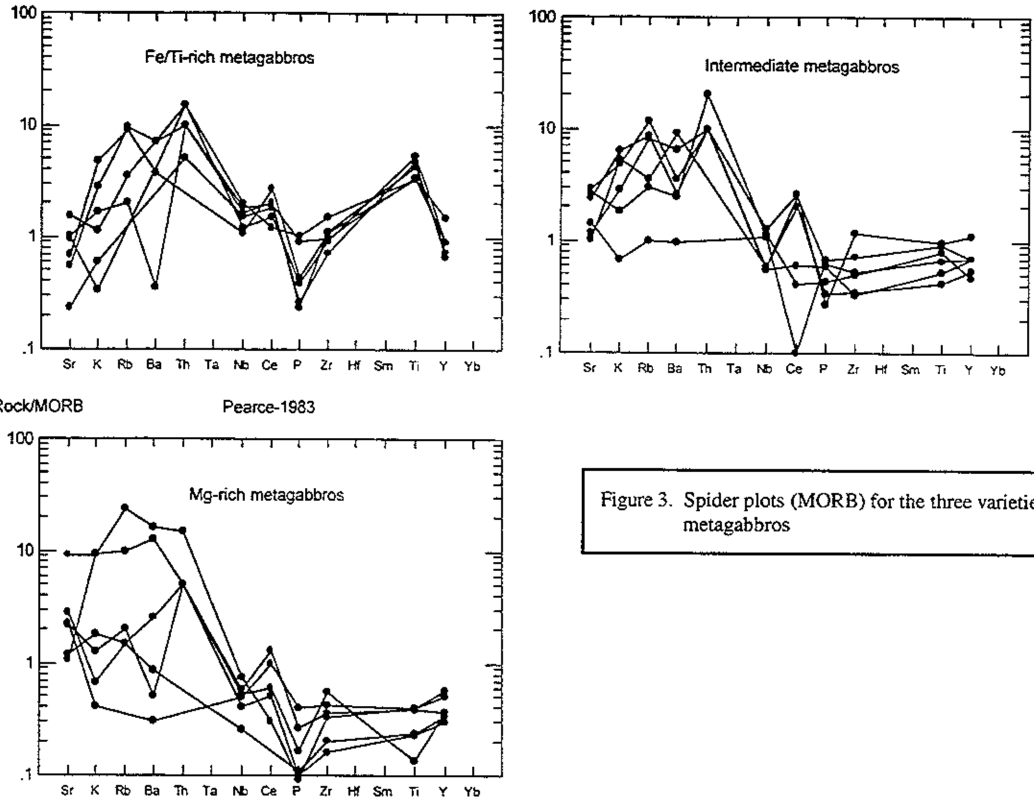

Figure 3. Spider plots (MORB) for the three varieties of metagabbros

Do These Rocks Represent Metamorphosed Gabbros? Comparing the bulk chemistry of the samples with the percentage weights of important oxides in the gabbro-diabase-basalt family which, according to Wahlstrom (1947), are approximately: SiO_2, 48.6; TiO_2, 1.2; Al_2O_3, 16.8; FeO (Fe^{2+} and Fe^{3+}), 10.4; Mg0, 6.8; CaO, 10; Na_2O, 2.8; and K_2O, 1.2, many similarities are seen. The silica content is found to be relatively high (~3%) in the intermediate metagabbros but is balanced out by lower values of aluminum.

Slight deviations from the normal values may be the result of fluid phases entering the rock during metamorphism. This is evident by the presence of felsic veins and bull quartz in the Fe/Ti-rich metagabbros near Ermoupoli. Further evidence is suggested by Schuling and Vink (1967) and Ernst (1972) from the occurrence of titanite vs the assemblage rutile-calcite-quartz in the cycladic blueschists, as well as much of the metagabbro samples collected on Syros.

Where These Rocks Originally Part of an Ophiolite Sequence? By examing the outcrops of Syros which are metagabbros, metabasalts, marbles, ultramafic melange zones with abundant serpentinite, and (in a localized area north of Ermoupoli) highly altered blueschists with relic patterns and textures of pillow basalt, the conclusion in made that these metagabbros belong to a metamorphosed ophiolite sequence. These units correlate well with the idealized ophiolite sequence, for example, in Liguria the mesozoic ophiolite sequence consists of serpentine, gabbro, pillow and massive basalts, together with breccia derived from these facies (Barrett and Spooner, 1977).

REFERENCES CITED.

Barrett, T.J. and Spooner, E.T.C. (1977): Ophiolitic breccias associated with allochthonous oceanic crustal rocks in the East Ligurian Apennines, Italy. Earth & Planetary Sci Lett., 35, 79-91.

Evans, B.W. (1986): Reactions among sodic, calcic, and ferromagnesian amphiboles, sodic pyroxenes, and deerite in high pressure metamorphosed ironstone, Siphnos, Greece. Amer Mineral. 71, 1118-1125.

Ernst, W.G. (1972): CO_2-poor compositions of the fluid attending Franciscan and Sanbagawa low-grade metamorphism. Geochim. Cosmochim. Acta, 36, 497-504.

Schuiling, R.D. (1973): In de Jong, K.A. & Schuilling R. (Eds), Gravity and Tectonics. Wiley, New York.

Schuiling, R.D. & Vink, B.W. (1967): Stability relations of some titanium minerals (sphene, perovskite, rutile, anatase). Geochim. Cosmochim. Acta, 31, 2399-2411

Wahlstrom, E. (1947): Igneous Minerals and Rocks. John Wiley and Sons Inc., New York.

Wilson, M. (1989): Igneous Petrogenesis: Unwin Hyman, New York.